

Establishing a microscopic model for nonfullerene organic solar cells: Self-accumulation effect of charges

Yao Yao

Citation: *J. Chem. Phys.* **149**, 194902 (2018); doi: 10.1063/1.5052656

View online: <https://doi.org/10.1063/1.5052656>

View Table of Contents: <http://aip.scitation.org/toc/jcp/149/19>

Published by the [American Institute of Physics](#)

PHYSICS TODAY

WHITEPAPERS

ADVANCED LIGHT CURE ADHESIVES

Take a closer look at what these environmentally friendly adhesive systems can do

READ NOW

PRESENTED BY
 **MASTERBOND**
ADHESIVES | SEALANTS | COATINGS

Establishing a microscopic model for nonfullerene organic solar cells: Self-accumulation effect of charges

Yao Yao^{a)}

Department of Physics and State Key Laboratory of Luminescent Materials and Devices,
South China University of Technology, Guangzhou 510640, China

(Received 20 August 2018; accepted 24 October 2018; published online 21 November 2018)

A one-dimensional many-body tight-binding model is established to mimic the charge distribution and dynamics in nonfullerene organic solar cells. Two essential issues are taken into account in the model: the alternating donor and acceptor structure, which is beneficial for the direct generation of charge transfer state, and the local imbalance of the intrinsic electrons and holes. The most remarkable outcome of the model is that, due to the strong Coulomb attractive potential energy, the intrinsic charges in the cells are self-accumulated in a small spatial region and outside the self-accumulation region the charge density vanishes so that the recombination is regarded to be largely suppressed. The photogenerated electrons are subsequently observed to spread freely outside the self-accumulation region, implying that the Coulomb attraction does not matter in the ultrafast charge separation dynamics. These findings enable the understanding of the high performance of emerging nonfullerene cells, and the designing rules of molecules and devices are then comprehensively discussed. *Published by AIP Publishing.* <https://doi.org/10.1063/1.5052656>

I. INTRODUCTION

Numerous research were devoted to nonfullerene organic solar cells (OSCs) in recent years due to their rapidly ever-growing performance.^{1–17} The up-to-date power conversion efficiency has achieved 17.3%,² greatly exceeding the long-lasting efficiency bottleneck for fullerene-based solar cells. The substantial progress benefits from two novel strategies. First, several nonfullerene acceptors (NFAs) based on the polycyclic aromatic hydrocarbon are utilized, such as the perylene and naphthalene, and their derivatives.¹⁷ These NFAs normally possess much smaller bandgap than that of fullerene so that the optical absorption of nonfullerene cells is much better than that of fullerene-based cells. Second, tandem structures are extensively employed so that the absorption of cells effectively covers the entire solar spectrum which further improves the efficiency.^{2,12,15} Despite the high device performance, the tandem structure is very complicated for a practical fabrication limiting its potential commercial applications. Researchers thus devoted great effort to the study of (cascade) multi-component blends, such as the donor/acceptor (D/A) binary blends and also the ternary ones with more complicated combinations of D and A components.^{17–31} The multi-component blends, both in all-polymer¹⁸ and all-small-molecule¹³ cells, perform as perfect as the tandem cells exhibiting promising application potentials in near future.

The physical origin of the driving force for the charge separation turned out to be a long-standing puzzle in OSCs.³² The relatively low dielectric constant of organic materials results in a strong Coulomb attractive potential energy between electrons and holes which is much stronger than that of the thermal

fluctuation and the built-in electric field, leading to the inefficient dissociation of photogenerated excitons. Therefore, in a long period of investigations on the OSCs, the acceptor has been generally chosen to be fullerene or its derivatives. The favorable molecular structure of the fullerene gives rise to plenty of available orbitals for electrons and thus the high electron affinity. In other words, in order to achieve enough driving force for the efficient charge separation, the fullerene-based cells compromise the optical absorption of acceptors by using fullerene with a wide energy gap. Due to the fixed gap of fullerene acceptors, the choice of donors is greatly limited. In order to improve the absorption and thus the short-circuit current (J_{sc}), the donors should be of low energy gap, and unfortunately, the energy offset of LUMO (lowest unoccupied molecular orbit) between the donor and acceptor is subsequently reduced, lowering the driving force of charge separation and thus the open-circuit voltage (V_{oc}). These two competing device operation parameters, J_{sc} and V_{oc} , constitute the bottleneck of the cell efficiency. Furthermore, it is reported that the wavefunction of electrons tends to be delocalized among the fullerene molecules and the charge separated states have larger density of states than that of local excitons.^{33–38} These two arguments are frequently employed to explain the mechanism of charge generation in fullerene-based cells. From these points of view, materials with better crystallinity or purity should perform better than the amorphous ones. In real situations, however, perylene derivatives with good crystallinity normally exhibit worse performance than other NFAs and ternary structured devices act as well as the binary ones,¹⁷ suggesting that the delocalization mechanism may not apply in these systems.

Nonfullerene cells extensively employ the “seem-to-be-poor” ternary structures and perform very well.¹⁷ They seem

^{a)}Electronic mail: yaoyao2016@scut.edu.cn

to be poor because the NFAs always have a relatively low bandgap so that in these structures the energy offset of HOMO (highest occupied molecular orbit) between the donor and acceptor, and thus, the driving force for hole transfer should be even smaller than that for the electron transfer in fullerene-based cells. A recent experiment has demonstrated that the driving force in nonfullerene cells is much smaller than that in fullerene-based cells,³⁹ which implies that the charge separation itself is a spontaneous process and does not need an energetic driving force. In the same experimental research, the J_{sc} is found to be largely improved by finely tuning the molecular structures while the V_{oc} is concurrently increased, which is in strong contrast to the situation in fullerene-based cells. As a result, the great achievements of nonfullerene cells are currently challenging the conventional theories for the charge separation in OSCs, and a comprehensive theoretical model applicable in this new kind of cells is greatly desirable.

For building a theoretical model that appropriately mimics the major physics in nonfullerene cells, we first distilled the following essential experimental findings up to date. First of all, due to the efficient absorption of photons in both donors and acceptors, the active layer is not necessarily to be very thick so that the charge carrier mobilities and thus the single-carrier transport properties do not essentially determine the device performance, while the charge separation still plays important roles for the device performance. Second, unlike the fullerene molecule, the NFAs always comprise complicated functional units which must be carefully considered. For example, the end groups manifest high electron affinity, and the side groups shaping the whole blend are of an alternating structure of D and A units. Finally, the existence of the polaron pair state as an important constituent of the photogenerated excited state has been demonstrated.^{40,41} The model in the present work will be established on the basis of these experimental facts. The paper is organized as follows. In Sec. II, we discuss the main features of nonfullerene cells and propose a model Hamiltonian to mimicking these cells. In Sec. III, the calculated results are present, and the self-accumulation effect and the ultrafast charge separation are investigated. The conclusion is drawn in Sec. IV with an outlook.

II. MICROSCOPIC MODEL

In this work, the blend of PBDB-T and ITIC is taken as the prototype to build our microscopic model.⁴² PBDB-T is a donor-type conjugated polymer consisting of a D–A structure with the D unit being BDT and the A unit being BDD.⁹ ITIC was first synthesized in 2015 and quickly became a benchmarking small-molecule NFA.⁵ It has an A–D–A structure with the core D unit being IDT and the two end units A being IC. The chemical structures of the molecules are displayed in Fig. 1(a). In this blend, the major electron-withdrawing groups should be the end groups of acceptor molecules, i.e., the cyano- and/or ketone-group in ICs.

The molecules used in the nonfullerene OSCs usually comprise three functional units.¹⁶ (1) The core groups, such as thiophene, perylene, the fused ring in ITIC, and the backbone in polymers, provide the main conjugated orbits for

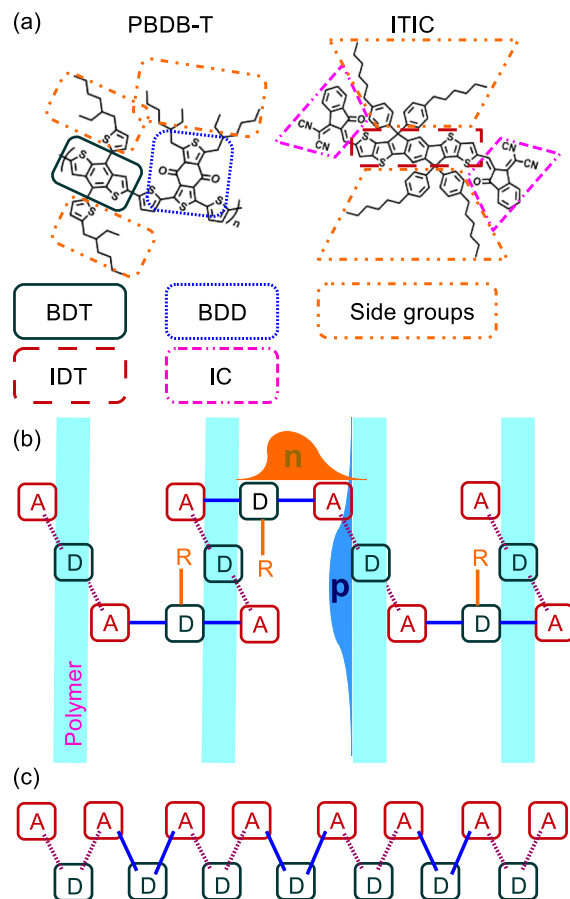


FIG. 1. (a) Chemical structures of PBDB-T and ITIC. (b) Model of an alternating structure of D and A units. The A–D–A structure of acceptor molecules is sandwiched between two polymer chains. The negative charges denoted by “n” are assumed to reside on the A unit of ITIC, while the positive charges denoted by “p” distribute along the polymer chain. “R” represents the side group. The solid lines represent the intramolecular bonds and the dashed lines denote the intermolecular interactions ($\pi - \pi$ stacking). (c) Schematic of the many-body tight-binding model abstracted from the real materials.

electrons and/or hole polarons. (2) The end groups with different electron affinities [and possibly some paired radicals (diradicals)^{43,44}] induce local charge dipoles which is the intrinsic charge transfer effect, and the imbalanced spatial distribution of negative and positive charges breaks the local neutrality in the device. For example, fluorine or the cyano-group has a strong ability of electron attraction, and experiments revealed that substitution with these groups can largely enhance the device performance.^{11,13} (3) The side groups with poor conductivity shape the special structure of the blend. Interestingly, one can find in Fig. 1(a) that there are long side groups on the D units in both PBDB-T and ITIC. These side groups form a scaffold which expands the molecules spatially, such that the D unit in PBDB-T does not directly get in contact to the D unit in ITIC.^{1,45} This means that the blend should be of a repeating structure of $D \cdots A-D-A \cdots$, with “ \cdots ” indicating the intermolecular contact and “ $-$ ” being the intramolecular bond. It is worth noting that the side group engineering is commonly employed in the fabrication of nonfullerene cells, implying that the alternating structure of D and A units may be essentially responsible for their high performance.¹⁶

As the first important ingredient in our model, the structure of the PBDB-T/ITIC heterojunction could be generally sketched as follows. The polymer chains of PBDB-T are parallel to each other, and the A–D–A structure of ITIC is sandwiched between two polymers with π – π stacking between the D unit of PBDB-T and the A unit of ITIC. This idea is inspired from the experimental fact which indicates that the good miscibility of ITIC and polymers leads to the ordered and uniform aggregation and the π – π stacking.⁵ The realistic situation could be slightly different because the polymer chains are always entangled, but this does not matter because the parallelism is not the central point of our simplified model. The side groups labeled by “R” in the D unit of ITIC separate the D units away from each other and shape a quasi-one-dimensional (1D) structure.

The dimensionality is an extensively discussed issue in OSCs. In the traditional fullerene-based cells, people believed that the fullerene molecules have a three-dimensional structure such that the entropy for free electron states in fullerene is much larger than that in polymer donors which have got low dimensionality.³² Being significantly different from fullerene, most commonly used small-molecule NFAs possess the planar structure and spatial anisotropy, suggesting that their dimensionality is smaller than 3 or even 2. There are two evidences. One is that the molecular orientation **and the domain purity** can largely influence the device performance of nonfullerene cells as stated by Hou *et al.*^{1,21} The other is the electron-spin resonance signal in ITIC exhibiting that the two radicals in ITIC form a local pair and excluding the possibility of the high-dimensional structure in which electrons are more delocalized.⁴⁴ With these considerations, we believe that our model is applicable to most planar NFAs. In addition, although the bulk heterojunction structure of OSCs leads to the amorphous phase, there is a 1D percolating pathway for the charge transport. We thus borrow this picture to mimic the nonfullerene solar cells with a quasi-1D microscopic model.

The second essential point introduced in the model is the local imbalanced charges while keeping charge neutrality of the whole cell. There are two origins of charges in the cells. The first one is the *intrinsic charge* self-doped by either electropolar (end) groups and/or radicals which can be self-accumulated in a small region as will be discussed in Sec. III.⁴³ The second one is the *photogenerated charge*. The photogenerated excited states have been demonstrated to comprise two components.^{40,41} One is the usual Frenkel exciton with local charge neutrality. More importantly, there is another elementary excitation, the charge transfer state (or the polaron pair state).⁴⁶ The charge transfer state consists of two spatially separated polarons with opposite charges. The excitations in the nonfullerene cells are thus the combinations of Frenkel excitons and polarons. We realize that the introduction of moieties with strong electron affinity such as the cyano-group and the alternating D and A structure can probably enhance the generation rate of polarons and thus the local imbalance of charges.

For convenience of description, in the following, we simply call the (intrinsic/photogenerated) negative charges as (intrinsic/photogenerated) electrons and the positive charges as holes. To avoid confusion, readers should bear in mind

that intrinsic and photogenerated electrons are indistinguishable particles according to the quantum statistical physics, but they have different origin. We assume that the intrinsic electrons locally reside on the A units of ITIC, while the intrinsic holes lie along the polymer chain due to the conjugation of polymers, as shown in Fig. 1(b). It means that some intrinsic holes distribute out of the range of the 1D alternating structure that we are investigating. As a result, the local density of electrons on the 1D alternating structure should be larger than that of holes. It is apparent that the opposite case could qualitatively produce the same conclusions. Furthermore, since we mainly consider the dynamics on an ultrafast time scale, the recombination terms will not be involved in the model. We will argue that due to the self-accumulation effect, the recombination in the realistic cells could be largely suppressed.

We are now on the stage to build the 1D tight-binding model with the geometrical structure schematized in Fig. 1(b). The solid lines in Fig. 1(b) represent the intramolecular covalence bonds in the ITIC molecules and the dashed lines denote the intermolecular interactions between PBDB-T and ITIC. Via the bridge effect of opposite units,^{47,48} holes move among the D units, while electrons move among the A units. As a normal consideration in tight-binding models, we assume that the hopping of holes or electrons can only occur between the nearest D or A unit, respectively, and for simplicity, we neglect the disorder of the hopping constant, which is beyond the scope of this work. Electrons and holes residing on nearest units will feel a strong attractive force which could be different for intra- and inter-molecular bond. We do not consider the long-range interaction because of the electrostatic screening of the opposite charges. It is worth noting that, if the long-range interaction is taken into account, the main conclusion in this work, i.e., the self-accumulation effect, would be further enhanced.

The Hamiltonian of the 1D alternating structure as schematized in Fig. 1(c) is thus written as

$$H = - \sum_j (t_e c_{2j}^\dagger c_{2j+2} + t_h d_{2j+1}^\dagger d_{2j+3} + \text{h.c.}) + \sum_j U_j c_{2j}^\dagger c_{2j} d_{2j+1}^\dagger d_{2j+1}, \quad (1)$$

where $c_{2j}^\dagger (c_{2j})$ creates (annihilates) an electron on $2j$ th site (unit); $d_{2j+1}^\dagger (d_{2j+1})$ creates (annihilates) a hole on $(2j + 1)$ th site; $t_{e/h}$ is the hopping constant for the electron/hole and we set them to 100 meV (on the order of vibrational frequencies) unless otherwise mentioned; U_j is the attractive potential energy between the nearest electron and hole. In order to distinguish the intra- and inter-molecular interactions, U_j for odd and even j will be set to different values U_1 and U_2 , respectively. For simplicity, we set U_1 to be -400 meV and adjust U_2 in the practical computations. It is reasonable that U_1 is at least four times larger than the hopping constant, since the dielectric constant in organic molecules is as small as 3 and the Coulomb interaction is relatively strong. We note here that, in realistic materials, the results could be quantitatively different from those presented in this work because of the distinct parameters and the neglect of the Coulomb repulsion

among like charges, but the qualitative conclusions are still valid.

One would be noting that, if we consider the electron as a spin up and the hole as a spin down, the model is nothing but a 1D extended Hubbard model with negative Hubbard U and next-nearest interactions. The features in the Luttinger liquid theory could be safely applied to the model. For example, with negative U , there is a phase named “phase separation” in which the charges are accumulated in a local region.⁴⁹ The self-accumulation effect actually stems from this effect. In addition, the Hubbard model and the Luttinger liquid theory have been applied to the benzene and fullerene systems,^{50,51} but these are solely related to single-component systems. Our model is more generic for multi-component cells.

III. RESULTS

In this section, we show the results calculated by the static and adaptive time-dependent density matrix renormalization group algorithm.^{52,53} The total number of sites in the system is set to 128, and the truncation number of states is 64. The key parameters are the total number of electrons and holes in the system, namely, N_e and N_h , respectively. Without loss of generality, we mainly study the case that the number of electrons is larger than that of holes in this work.

A. Self-accumulation effect of intrinsic charges

We first study the properties of the intrinsic charges of the system without photoexcitation. The local charge densities $\rho_{e/h}(x, t)$ for electrons (minus sign) or holes (positive sign) with x being the site index are calculated with $N_h = 6$, $U_2 = -200$ meV, and different N_e , as shown in Fig. 2. It is found that when $N_e \leq 10$, the intrinsic charges are accumulated in

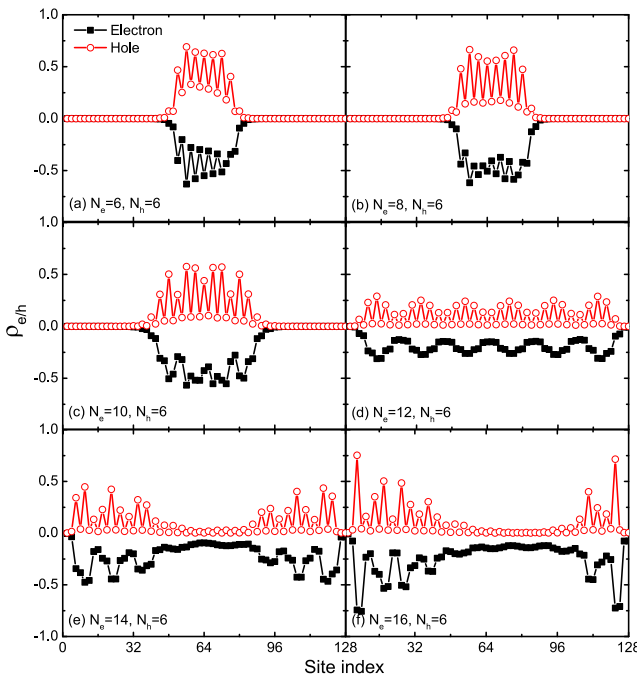


FIG. 2. Charge densities $\rho_{e/h}$ on the lattice for $N_h = 6$, $U_2 = -200$ meV, and six sets of N_e .

a small spatial region of the lattice and outside the region the charge densities are completely vanishing. For example, in the case $N_e = 8$, the charge densities are accumulated within 40 sites. Holes are spaced out over 20 sites, while electrons are approximately evenly distributed, since now the total number of electrons is larger than that of holes. As stated, this is the feature of the phase separation of intrinsic charges.⁴⁹ The strong Coulomb attraction between electrons and holes results in the accumulation. In organic materials, due to the small dielectric constant, the Coulomb attraction is always sufficiently strong so that the accumulation found here could be spontaneously present in realistic cases. Intrinsic charges in the vicinity are easily absorbed into the accumulation region making the vicinity region empty. We call this effect “self-accumulation,” which is one of the essential consequences of this work. When $N_e > 10$, the self-accumulation effect breaks down and the system enters the phase of the charge density wave.

We can parallelly calculate the cases of other values of N_h , and Fig. 3 displays a phase diagram to figure out the parameter regimes for the appearance of self-accumulation effect. Obviously, when the intrinsic electrons and holes are nearly equivalent, namely, $N_e \approx N_h$, the self-accumulation effect emerges as expected. The phase boundaries are close to linear and located at around $N_e/N_h = N_h/N_e \approx 1.75$. One can see that the parameter regime for the self-accumulation effect is quite flexible. It is not necessary that the electron density is extremely larger than that of holes, so a number of organic materials can be chosen as candidates for the non-fullerene cells. As discussed later, however, if N_e is very close to N_h , the photogenerated charges are not easy to be dissociated. Subsequently, we conclude here an optimal condition for an efficient nonfullerene cell is that N_e/N_h or N_h/N_e lies between 1.5 and 2.0, depending on the specific material parameters.

As a critical consequence, the self-accumulation effect of intrinsic charges stems from the alternating D and A structure. As aforementioned, this effect leads to the suppression of charge recombination, since there are few charges outside the self-accumulation region. It is well accepted that the nonfullerene cells manifest good performance, but people do not understand why the ultrahigh recombination loss of V_{oc}

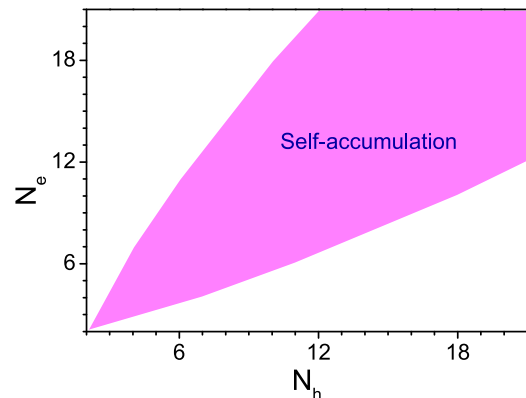


FIG. 3. Phase diagram of the model for $U_2 = -200$ meV and different sets of N_e and N_h . The purple area illustrates the self-accumulation phase.

observed in traditional fullerene-based cells is suppressed in this new kind of cells.^{54,55} Herein, we provide a possible explanation of this issue by uncovering the self-accumulation effect of intrinsic charges.

B. Spread of photogenerated charges outside the self-accumulation region

In this subsection, we calculate the dynamics upon photoexcitation. As shown in Fig. 3, for $N_h = 6$, the phase boundary of self-accumulation locates at $N_e \simeq 10$. For mimicking the physical situation of photoexcitation, we fix N_h to be 6 and set N_e to be larger than 10, which is the maximum number of intrinsic electrons for the presence of self-accumulation as discussed in Subsection III A, and the excess electrons over the 10 intrinsic electrons are thus regarded to be photogenerated. At time $t \leq 0$, we add a balance potential energy to the system for both electrons and holes with the form being $V(x) = -0.5 \exp[-(x - x_c)^2/400]$ with x_c being the center of the lattice. In this situation, the electrons and holes will be initially accumulated in the middle of the lattice. Once time $t > 0$, the potential is switched off to mimic the situation that the laser pulse is switched off and afterward the photogenerated electrons start to spread. We then calculate $\Delta\rho_{e/h}[\equiv\rho_{e/h}(t) - \rho_{e/h}(0)]$ to quantify the spreading charges.

In Fig. 4, the spatial and temporal dependences of both $\Delta\rho_{e/h}$ and $\rho_{e/h}$ are shown with $N_e = 14$, $N_h = 6$, and $U_2 = -200$ meV. As expected, both the electrons and holes are initially accumulated in the middle of the system due to the initial potential energy. After the initial potential is off, it is found that a part of electrons which can be regarded as photogenerated electrons quickly spread out to the two ends of the lattice. At around 100 fs, the photogenerated electron wavepackets travel over 40 sites and arrive in the ends, and then they will stay there as we do not consider the recombination loss. In a realistic situation, 40 sites are long enough for the electron-hole pair to be dissociated. In order to maintain the conservation of the particle number in the entire system, in the middle of the lattice, two positive peaks are induced which do not move during the whole process. The summation of the density of spreading photogenerated electrons at 100 fs equals to 1.89, which means about $2e$ spread out of the self-accumulation region. On the other hand, one can find that the hole density (red dashed lines in Fig. 4) does not almost change at all. This is surprising because we expected that the spreading electrons would be able to pull at least a few holes out due to the strong attraction among them. It suggests a new mechanism for the charge separation of photogenerated electron-hole pairs. As stated, when $N_e \leq 10$, the intrinsic charges are self-accumulated so that $10e$ are recognized to be resident charges self-doped by electropolar groups and/or radicals. The other electrons could therefore be regarded to be originated from photogeneration, and 2 of them spontaneously leave the self-accumulation region leading to an effective dissociation of the electron-hole pairs and ultrafast charge separation process. This effect turns out to be the second remarkable finding in this work.

In order to see the essential parameters affecting the motion of photogenerated electrons and holes, we adjust the

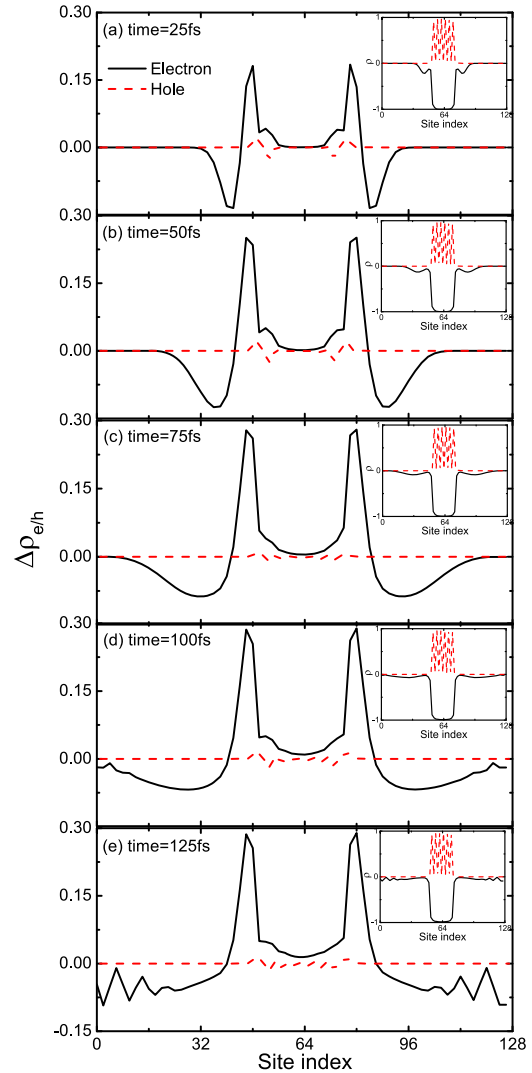


FIG. 4. Spatial distribution of $\Delta\rho_{e/h}$ at five time points. The insets show the relevant distribution of charge densities $\rho_{e/h}$. The parameters are $N_e = 14$, $N_h = 6$, and $U_2 = -200$ meV.

total number of electrons N_e while keeping N_h to be 6. It is found in Fig. 5 that when $N_e = 12$, the spread of photogenerated electrons is extremely slow. When $N_e \geq 14$, the spread becomes efficient, and the larger the N_e is, the faster the spread is. As a comparison, the time evolution of hole density is plotted in Fig. 6, where one can observe that the hole density does not almost spread in the entire process. Notice that in our model, we do not consider any energy offsets and energetic driving forces; this could be regarded as a novel scenario of charge separation in the presence of strong Coulomb attraction between electrons and holes. We also calculate the time evolution for different U_2 and $t_{e/h}$ and the results are shown in Fig. 7. Following the increase in U_2 , the region of self-accumulation becomes shrunk, while the motion of photogenerated electrons outside the region is not affected. With $t_{e/h}$ decreasing, the spreading velocity of electrons reduces as expected. In our model, U_2 is an adjustable phenomenological parameter to denote the intermolecular Coulomb attraction. It also quantifies the binding energy of the intermolecular charge transfer state which is essential in the charge separation process. The driving force of the dissociation of the charge transfer state

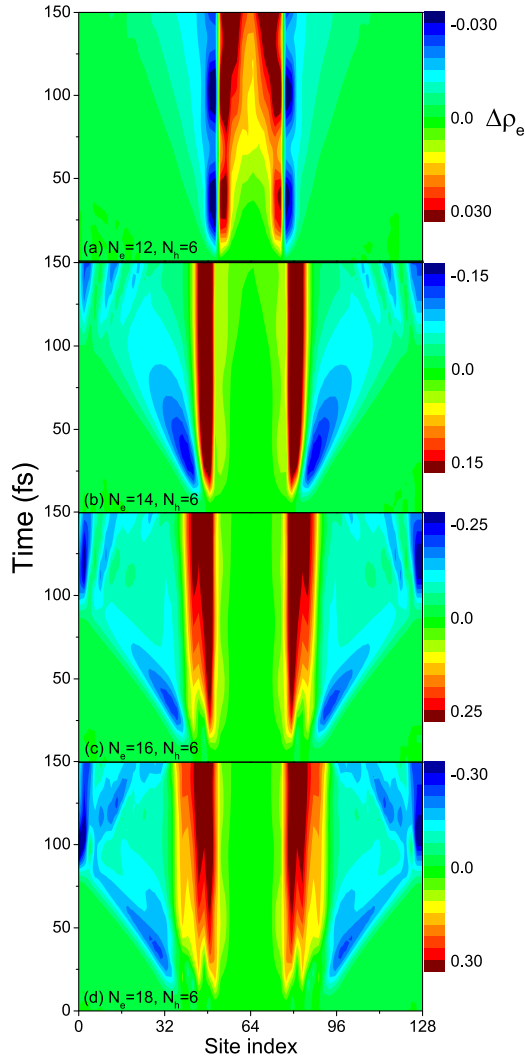


FIG. 5. Time evolution of $\Delta\rho_e$ on the lattice for four sets of N_e and $N_h = 6$, and $U_2 = -200$ meV.

serves as a long-term research subject in the community. In particular, when the binding energy is very strong, the dissociation is regarded to be difficult. Here, our results provide an alternative understanding of this issue: If there is a self-accumulated region, the binding energy does not matter in the charge separation.

As an additional remark, the ultrafast charge separation process presented here is completely different from that in

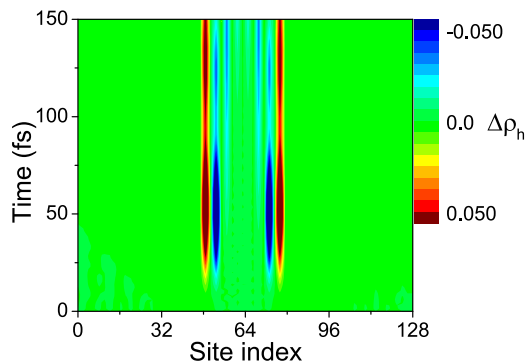


FIG. 6. Time evolution of $\Delta\rho_h$ on the lattice for $N_e = 16$, $N_h = 6$, and $U_2 = -200$ meV.

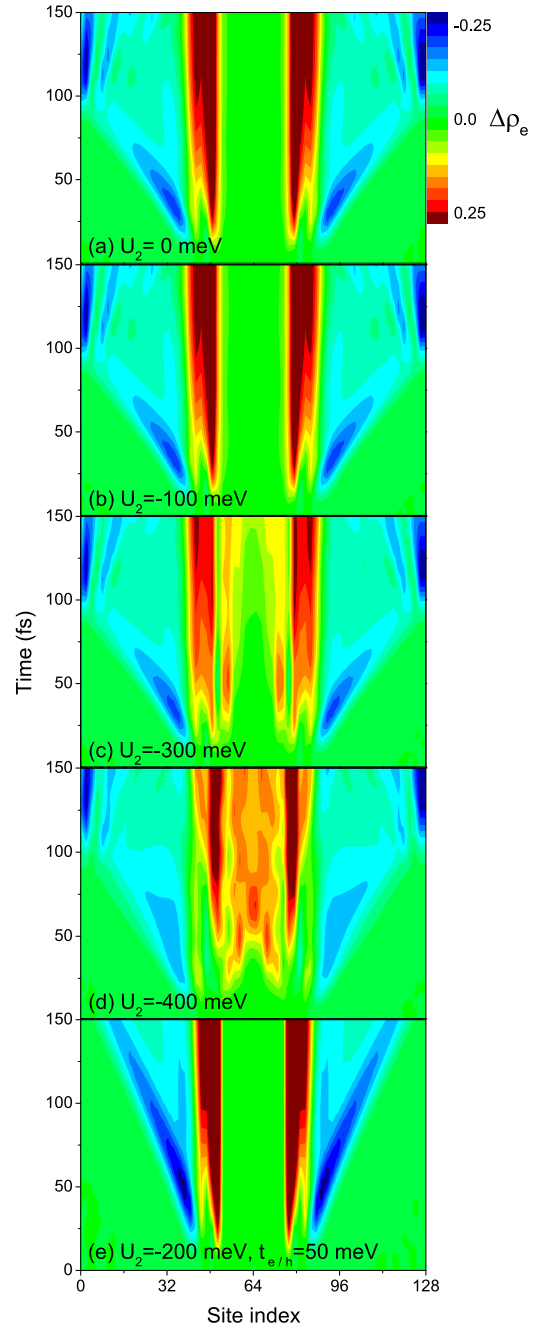


FIG. 7. Time evolution of $\Delta\rho_e$ on the lattice for five sets of U_2 and $t_{e/h}$ and $N_e = 16$, and $N_h = 6$.

the planar heterojunctions which is correlated with the long-range charge transfer state.³⁸ In the latter case, there is not an alternating structure so that the many-body model cannot be applied and the self-accumulation effect cannot be found. As we studied in the previous work, a nonlocal electron-phonon interaction is necessary to serve as the driving force for the charge separation.³⁸ In the present model, the electron-phonon interaction is not taken into account and the driving force turns out to be the many-body effect of electrons and holes.

C. Photogenerated charge transport outside the self-accumulation region

As the photogenerated electrons will spontaneously spread out of the self-accumulation region, one would be

wondering what will happen when these photogenerated electrons encounter the other self-accumulation region: Will they be absorbed by this region due to the strong Coulomb attraction? If the answer is yes, it means that the recombination loss of photogenerated charges is still large in the cells. In order to mimic the physical scenario, in the presence of $V(x)$, an additional term $\tilde{V}_{e/h}$ is initially acted on the site $x_c - 25$ on which local electron/hole densities are induced. To distinguish the behavior of electrons and holes, $\tilde{V}_{e/h}$ is adjusted to be different values for electrons and holes such that we can separately study the motion of photogenerated electrons and holes and eliminate the influence of the interaction between them.

Figure 8 shows the evolution of $\rho_{e/h}$ for $N_e = 14$, $N_h = 6$, and $U_2 = -200$ meV. In order to be more focused, only 48 sites are displayed. As indicated by the arrows, there is a local excitation of the electron/hole charge density outside the self-accumulation region, and as time evolves, the charges split into two branches and spread to opposite directions. For electrons, the right-moving branch runs and crashes against the self-accumulation region, and it quickly rebounds to the left. It means that the photogenerated electrons are not captured by the accumulated charges, suggesting that the photogenerated electrons are nearly free and have minimal chance to be captured and recombined. On the other hand, the holes behave different as one can find in Fig. 8(b) that the majority hole densities are localized adhering to the self-accumulation region, implying that the holes are easy to be captured. This is easy to understand since we are studying the case where the electrons play a major role. As a result, so long as the local density of electrons is larger than that of holes, they can be efficiently separated and the electrons can be smoothly transported out of the active layer.

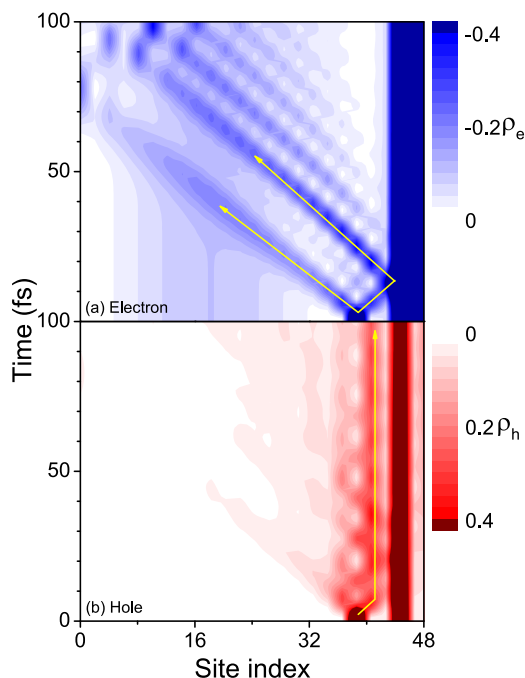


FIG. 8. Time evolution of $\rho_{e/h}$ on the lattice for $N_e = 14$, $N_h = 6$, and $U_2 = -200$ meV. The arrows indicate the paths of electrons and holes.

IV. CONCLUSION AND OUTLOOK

In summary, we have presented a 1D many-body microscopic model taking the strong Coulomb attraction between electrons and holes into account. By the analysis of the molecular structures of PBDB-T and ITIC, an alternating D and A structure is proposed which gives rise to an efficient generation of charge transfer states. It is found that there is a self-accumulation region in the electron-rich case and outside the region there are few charges leading to free transport of photogenerated electrons. In a dynamical manner, the photogenerated electron is uncovered to be easily dissociated from the self-accumulation region. We realize that this effect could be applied to explain the underlying mechanism of ultrafast charge separation in multi-component nonfullerene OSCs.

As an outlook, we would like to discuss more on the designing rules of OSCs. As stated, fullerene molecules possess denser states for electrons and higher symmetry than other organic molecules so that in a long history the fullerene dominated the battles among electron acceptors. Fullerene molecules however hold a very obvious drawback, i.e., its energy gap is very wide to absorb the solar emission. This drawback constrains the choice of donor materials which must be of low energy gap and the choice of the device structure in which the donor layer must be sufficiently thick. As a result, both the V_{oc} and J_{sc} easily meet their bottlenecks in the fullerene-based cells. In the early studies of NFAs, the designing rule suitable for the fullerene is also partly applied to the NFAs which slows down the developing progress.

Based upon the new insights of nonfullerene cells, the designing rules should also be modified to a large extent. Here, we summarize two sufficient conditions for an efficient charge separation in the cells. (1) An alternating structure of D and A units is essential. The reason is twofold. First, the D–A structure prefers the charge transfer states rather than Frenkel excitons, which means that in this structure the charge transfer states are more easily to be generated than in other structures. Second, as found in this work, the D and A alternating structure gives rise to self-accumulation of charges implying that outside the region there are few charges. As stated, this is critically important because the recombination outside the accumulated region is overwhelmingly weakened such that the transporting electrons outside the accumulated region can be smoothly collected by the electrodes. This can be adopted to explain the reason that the V_{oc} loss is not significant in nonfullerene cells.³⁹ On the experimental side, the alternating structure could be achieved by either properly modulating the side groups or adding strong electropolar groups to firmly connect the D and A units. In our work, we take a 1D structure as an example, but a 2D structure still works because the 2D system also shares the features of the Luttinger liquid. (2) There has to be imbalanced local charge densities of intrinsic electrons and holes. A certain amount of intrinsically self-doped charges are essential for the cells,⁴⁴ and in a local system with an equal number of electrons and holes, the mechanism does not work as stated. We guess that the self-doping and thus the self-accumulation effect may stem from

spontaneous delocalization of radicals, which needs further experimental evidences. On the other hand, the imbalance of charges may not be easy to be measured, but we think that it is possible to detect the magnetic domain induced by the self-accumulated electrons and holes (diradicals). Apart from these two issues, the electronic energies (to form the cascade structure) and the molecular morphology (to form a percolating pathway for charge transport) do not play the significant role, opposite to the conventional viewpoint in fullerene-based cells.

In addition, our model can be straightforwardly applied to other nonfullerene cells besides the PBDB-T/ITIC blend. It is not necessary to require a NFA to have the similar A-D-A structure with that in ITIC. Proper modulation of side groups can still shape the alternating structure and a large difference of electron affinity can enhance the packing of the D and A units. Rather, the parameters for efficient charge separation must be reconfirmed in other cells.

1D metal exhibits the feature of the Luttinger liquid, and one important phenomenon in 1D metals is the so-called spin-charge separation.^{52,53} That is, in a non-half-filled Hubbard model with on-site repulsive interaction, it is well known that the charge excitation moves faster than spin. The present mechanism of charge separation is however different from the spin-charge separation, since we do not find the spread of holes. In addition, the electron-phonon interaction and the disorders are always essential in organic materials. Taking both the electron-phonon interactions and disorder into account, it refers to the effect of many-body localization.⁵⁶ We expect that the many-body localization can enhance the present self-accumulation effect since in this situation the charges are more likely to be localized. This will be taken as the future subject.

ACKNOWLEDGMENTS

The authors gratefully acknowledge support from the National Natural Science Foundation of China (Grant Nos. 11574052 and 91333202). We thank Professors Jianhui Hou, Haibo Ma, Yuanping Yi, and Yuan Li for fruitful discussions and Wenchao Yang for proofreading the manuscript.

- ¹For a review, see J. Hou, O. Inganäs, R. H. Friend, F. Gao, *Nat. Mater.* **17**, 119 (2018).
- ²L. Meng, Y. Zhang, X. Wan, C. Li, X. Zhang, Y. Wang, X. Ke, Z. Xiao, L. Ding, R. Xia, H.-L. Yip, Y. Cao, and Y. Chen, *Science* **361**, 1094 (2018).
- ³B. Kan, Q. Zhang, M. Li, X. Wan, W. Ni, G. Long, Y. Wang, X. Yang, H. Feng, and Y. Chen, *J. Am. Chem. Soc.* **136**, 15529 (2014).
- ⁴Q. Zhang, B. Kan, F. Liu, G. Long, X. Wan, X. Chen, Y. Zuo, W. Ni, H. Zhang, M. Li, Z. Hu, F. Huang, Y. Cao, Z. Liang, M. Zhang, T. P. Russell, and Y. Chen, *Nat. Photonics* **9**, 35 (2015).
- ⁵Y. Lin, J. Wang, Z.-G. Zhang, H. Bai, Y. Li, D. Zhu, and X. Zhan, *Adv. Mater.* **27**, 1170 (2015).
- ⁶Y. Lin, Z.-G. Zhang, H. Bai, J. Wang, Y. Yao, Y. Li, D. Zhu, and X. Zhan, *Energy Environ. Sci.* **8**, 610 (2015).
- ⁷Y. Lin, Q. He, F. Zhao, L. Huo, J. Mai, X. Lu, C.-J. Su, T. Li, J. Wang, J. Zhu, Y. Sun, C. Wang, and X. Zhan, *J. Am. Chem. Soc.* **138**, 2973 (2016).
- ⁸Y. Lin, F. Zhao, Q. He, L. Huo, Y. Wu, T. C. Parker, W. Ma, Y. Sun, C. Wang, D. Zhu, A. J. Heeger, S. R. Marder, and X. Zhan, *J. Am. Chem. Soc.* **138**, 4955 (2016).
- ⁹W. Zhao, D. Qian, S. Zhang, S. Li, O. Inganäs, F. Gao, and J. Hou, *Adv. Mater.* **28**, 4734 (2016).
- ¹⁰M. Li, K. Gao, X. Wan, Q. Zhang, B. Kan, R. Xia, F. Liu, X. Yang, H. Feng, W. Ni, Y. Wang, J. Peng, H. Zhang, Z. Liang, H.-L. Yip, X. Peng, Y. Cao, and Y. Chen, *Nat. Photonics* **11**, 85 (2017).

- ¹¹W. Zhao, S. Li, H. Yao, S. Zhang, Y. Zhang, B. Yang, and J. Hou, *J. Am. Chem. Soc.* **139**, 7148 (2017).
- ¹²Y. Cui, H. Yao, B. Gao, Y. Qin, S. Zhang, B. Yang, C. He, B. Xu, and J. Hou, *J. Am. Chem. Soc.* **139**, 7302 (2017).
- ¹³B. Qiu, L. Xue, Y. Yang, H. Bin, Y. Zhang, C. Zhang, M. Xiao, K. Park, W. Morrison, Z.-G. Zhang, and Y. Li, *Chem. Mater.* **29**, 7543 (2017).
- ¹⁴H. Yao, D. Qian, H. Zhang, Y. Qin, B. Xu, Y. Cui, R. Yu, F. Gao, and J. Hou, *Chin. J. Chem.* **36**, 491 (2018).
- ¹⁵Y. Cui, H. Yao, C. Yang, S. Zhang, and J. Hou, *Acta Polym. Sin.* **2018**(2), 223–230 (2017).
- ¹⁶S. Dai and X. Zhan, *Acta Polym. Sin.* **2017**(11), 1706–1714.
- ¹⁷X. Liu, Y. Yan, Y. Yao, and Z. Liang, *Adv. Funct. Mater.* **28**, 1802004 (2018).
- ¹⁸W. Su, Q. Fan, X. Guo, B. Guo, W. Li, Y. Zhang, M. Zhang, and Y. Li, *J. Mater. Chem. A* **4**, 14752 (2016).
- ¹⁹D. Baran, R. S. Ashraf, D. A. Hanifi, M. Abdelsamie, N. Gasparini, J. A. Röhr, S. Holliday, A. Wadsworth, S. Lockett, M. Neophytou, C. J. M. Emmott, J. Nelson, C. J. Brabec, A. Amassian, A. Salleo, T. Kirchartz, J. R. Durrant, and I. McCulloch, *Nat. Mater.* **16**, 363 (2017).
- ²⁰W. Zhao, S. Li, S. Zhang, X. Liu, and J. Hou, *Adv. Mater.* **29**, 1604059 (2017).
- ²¹H. Zhang, X. Wang, L. Yang, S. Zhang, Y. Zhang, C. He, W. Ma, and J. Hou, *Adv. Mater.* **29**, 1703777 (2017).
- ²²R. Yu, S. Zhang, H. Yao, B. Guo, S. Li, H. Zhang, M. Zhang, and J. Hou, *Adv. Mater.* **29**, 1700437 (2017).
- ²³C. Wang, X. Xu, W. Zhang, S. B. Dkhil, X. Meng, X. Liu, O. Margeat, A. Yartsev, W. Ma, J. Ackermann, E. Wang, and M. Fahlman, *Nano Energy* **37**, 24 (2017).
- ²⁴Y. Chen, Y. Qin, Y. Wu, C. Li, H. Yao, N. Liang, X. Wang, W. Li, W. Ma, and J. Hou, *Adv. Energy Mater.* **7**, 1700328 (2017).
- ²⁵M. An, F. Xie, X. Geng, J. Zhang, J. Jiang, Z. Lei, D. He, Z. Xiao, and L. Ding, *Adv. Energy Mater.* **7**, 1602509 (2017).
- ²⁶L. Zhong, L. Gao, H. Bin, Q. Hu, Z.-G. Zhang, F. Liu, T. P. Russell, Z. Zhang, and Y. Li, *Adv. Energy Mater.* **7**, 1602215 (2017).
- ²⁷B. Fan, W. Zhong, X.-F. Jiang, Q. Yin, L. Ying, F. Huang, and Y. Cao, *Adv. Energy Mater.* **7**, 1602127 (2017).
- ²⁸W. Zhong, J. Cui, B. Fan, L. Ying, Y. Wang, X. Wang, G. Zhang, X.-F. Jiang, F. Huang, and Y. Cao, *Chem. Mater.* **29**, 8177 (2017).
- ²⁹X. A. Jeanbourquin, A. Rahmanudin, X. Yu, M. Johnson, N. Guijarro, L. Yao, and K. Sivula, *ACS Appl. Mater. Interfaces* **9**, 27825 (2017).
- ³⁰N. Zhu, W. Zhang, Q. Yin, L. Liu, X. Jiang, Z. Xie, and Y. Ma, *ACS Appl. Mater. Interfaces* **9**, 17265 (2017).
- ³¹L. Yang, W. Gu, L. Hong, Y. Mi, F. Liu, M. Liu, Y. Yang, B. Sharma, X. Liu, and H. Huang, *ACS Appl. Mater. Interfaces* **9**, 26928 (2017).
- ³²T. M. Clarke and J. R. Durrant, *Chem. Rev.* **110**, 6736 (2010).
- ³³A. A. Bakulin, A. Rao, V. G. Pavelyev, P. H. M. van Loosdrecht, M. S. Pshenichnikov, D. Niedzialek, J. Cornil, D. Beljonne, and R. H. Friend, *Science* **335**, 1340 (2012).
- ³⁴A. Rao, P. C. Y. Chow, S. Gelinias, C. W. Schlenker, C. Z. Li, H. L. Yip, A. K.-Y. Jen, D. S. Ginger, and R. H. Friend, *Nature* **500**, 435 (2013).
- ³⁵S. Gelinias, A. Rao, A. Kumar, S. L. Smith, A. W. Chin, J. Clark, T. S. van der Poll, G. C. Bazan, and R. H. Friend, *Science* **343**, 512 (2014).
- ³⁶S. M. Falke, C. A. Rozzi, D. Brida, M. Maiuri, M. Amato, E. Sommer, A. De Sio, A. Rubio, G. Cerullo, E. Molinari, and C. Lienau, *Science* **344**, 1001 (2014).
- ³⁷B. A. Gregg, *J. Phys. Chem. Lett.* **2**, 3013 (2011).
- ³⁸Y. Yao, X. Xie, and H. Ma, *J. Phys. Chem. Lett.* **7**, 4830 (2016).
- ³⁹J. Liu, S. Chen, D. Qian, B. Gautam, G. Yang, J. Zhao, J. Bergqvist, F. Zhang, W. Ma, H. Ade, O. Inganäs, K. Gundogdu, F. Gao, and H. Yan, *Nat. Energy* **1**, 1 (2016).
- ⁴⁰A. De Sio, F. Troiani, M. Maiuri, J. Réhault, E. Sommer, J. Lim, S. F. Huelga, M. B. Plenio, C. A. Rozzi, G. Cerullo, E. Molinari, and C. Lienau, *Nat. Commun.* **7**, 13742 (2016).
- ⁴¹R. Wang, Y. Yao, C. Zhang, Y. Zhang, Z. Zhang, X. Xie, H. Ma, X. Wang, Y. Li, and M. Xiao, "Ultrafast hole transfer mediated by polaron pairs in an all-polymer photovoltaic blend" (to be published).
- ⁴²PBDB-T is the abbreviation of poly[(2,6-(4,8-bis(5-(2-ethylhexyl)thiophen-2-yl)-benzo[1,2-b:4,5-b']dithiophene))-alt-(5,5-(1,3-di-2-thienyl-5,7-bis(2-ethylhexyl)benzo[1,2-c:4,5-c']dithiophene-4,8-dione))] and ITIC is the abbreviation of (3,9-bis(2-methylene-(3-(1,1-dicyanomethylene)-indanone))-5,5,11,11-tetrakis(4-hexylphenyl)-dithieno[2,3-d':2,3-d]-s-indaceno[1,2-b:5,6-b']dithiophene).

- ⁴³Z. Wang, N. Zheng, W. Zhang, H. Yan, Z. Xie, Y. Ma, F. Huang, and Y. Cao, *Adv. Energy Mater.* **7**, 1700232 (2017).
- ⁴⁴Y. Li, L. Li, Y. Wu, and Y. Li, *J. Phys. Chem. C* **121**, 8579 (2017).
- ⁴⁵J. Hou, private communication (2018).
- ⁴⁶In polymers, the charge transfer state is more likely to be the polaron pair state.^{40,41} Due to the strong vibronic couplings, in small molecules, we can also call the electrons and holes as negative and positive charged (small) polarons. In this manner, the charge transfer state in small molecules can be regarded as equivalent to the polaron pair state.
- ⁴⁷H. Geng, X. Zheng, Z. Shuai, L. Zhu, and Y. Yi, *Adv. Mater.* **27**, 1443 (2015).
- ⁴⁸G. Li, N. Govind, M. A. Ratner, C. J. Cramer, and L. Gagliardi, *J. Phys. Chem. Lett.* **6**, 4889 (2015).
- ⁴⁹S.-J. Gu, S.-S. Deng, Y.-Q. Li, and H.-Q. Lin, *Phys. Rev. Lett.* **93**, 086402 (2004).
- ⁵⁰M. Schüler, M. Rösner, T. O. Wehling, A. I. Lichtenstein, and M. I. Katsnelson, *Phys. Rev. Lett.* **111**, 036601 (2013).
- ⁵¹H. Yoshioka, H. Shima, Y. Noda, S. Ono, and K. Ohno, *Phys. Rev. B* **93**, 165431 (2016).
- ⁵²C. Kollath, U. Schollwöck, and W. Zwerger, *Phys. Rev. Lett.* **95**, 176401 (2005).
- ⁵³Y. Yao, H. Zhao, J. E. Moore, and C.-Q. Wu, *Phys. Rev. B* **78**, 193105 (2008).
- ⁵⁴J. Yao, T. Kirchartz, M. S. Vezie, M. A. Faist, W. Gong, Z. He, H. Wu, J. Troughton, T. Watson, D. Bryant, and J. Nelson, *Phys. Rev. Appl.* **4**, 014020 (2015).
- ⁵⁵W. Yang, Y. Luo, P. Guo, H. Sun, and Y. Yao, *Phys. Rev. Appl.* **7**, 044017 (2017).
- ⁵⁶P. Bordia, H. P. Lüschen, S. S. Hodgman, M. Schreiber, I. Bloch, and U. Schneider, *Phys. Rev. Lett.* **116**, 140401 (2016).